

# Geophysical Research Letters

## RESEARCH LETTER

10.1029/2021GL092395

### Special Section:

The COVID-19 pandemic: linking health, society and environment

### Key Points:

- PM<sub>2.5</sub> pollution in Shanghai were mostly attributed to the regional transport carried by frequent westerly winds during the COVID-lockdown
- The transport contributed aerosols in Shanghai are less affected by the lockdown measures due to the less decreased surrounding emissions
- Synergetic emission control measures, especially those on ammonia emissions, are effective in mitigating the adverse transport impacts

### Supporting Information:

Supporting Information may be found in the online version of this article.

### Correspondence to:

J. Xu and Y. Duan,  
[metxujm@163.com](mailto:metxujm@163.com);  
[duanys@sheemc.cn](mailto:duanys@sheemc.cn)



### Citation:

Gu, Y., Yan, F., Xu, J., Duan, Y., Fu, Q., Qu, Y., & Liao, H. (2021). Mitigated PM<sub>2.5</sub> changes by the regional transport during the COVID-19 lockdown in Shanghai, China. *Geophysical Research Letters*, 48, e2021GL092395. <https://doi.org/10.1029/2021GL092395>

Received 6 JAN 2021  
 Accepted 31 MAR 2021

© 2021. American Geophysical Union.  
 All Rights Reserved.

## Mitigated PM<sub>2.5</sub> Changes by the Regional Transport During the COVID-19 Lockdown in Shanghai, China

Yixuan Gu<sup>1,2</sup> , Fengxia Yan<sup>3</sup>, Jianming Xu<sup>1,2</sup>, Yusen Duan<sup>4</sup>, Qingyan Fu<sup>4</sup>, Yuanhao Qu<sup>1,2</sup>, and Hong Liao<sup>5</sup> 

<sup>1</sup>Shanghai Typhoon Institute, China Meteorological Administration, Shanghai, China, <sup>2</sup>Shanghai Key Laboratory of Meteorology and Health, Shanghai Meteorological Service, Shanghai, China, <sup>3</sup>East China Air Traffic Management Bureau, Shanghai, China, <sup>4</sup>Shanghai Environmental Monitoring Center, Shanghai, China, <sup>5</sup>Jiangsu Collaborative Innovation Center of Atmospheric Environment and Equipment Technology, Jiangsu Key Laboratory of Atmospheric Environment Monitoring and Pollution Control, School of Environmental Science and Engineering, Nanjing University of Information Science and Technology, Nanjing, China

**Abstract** Intensive observations and WRF-Chem simulations are applied in this study to investigate the adverse impacts of regional transport on the PM<sub>2.5</sub> (fine particulate matter; diameter  $\leq 2.5 \mu\text{m}$ ) changes in Shanghai during the Coronavirus Disease 2019 lockdown. As the local atmospheric oxidation capacity was observed to be generally weakened, strong regional transport carried by the frequent westerly winds is suggested to be the main driver of the unexpected pollution episodes, increasing the input of both primary and secondary aerosols. Contributing 40%–80% to the PM<sub>2.5</sub>, the transport contributed aerosols are simulated to exhibit less decreases (13.2%–21.8%) than the local particles (37.1%–64.8%) in urban Shanghai due to the lockdown, which largely results from the less decreased industrial and residential emissions in surrounding provinces. To reduce the influence of the transport, synergetic emission control, especially synergetic ammonia control, measures are proved to be effective strategies, which need to be considered in future regulations.

**Plain Language Summary** The anthropogenic emissions were sharply reduced in China due to the lockdown measures during the Coronavirus Disease 2019 pandemic. However, the reduced emissions did not lead to expected decreases in fine particulate matter in Shanghai. To understand why haze pollution still occurred during the lockdown, intensive observations and a variety of simulations using the regional chemical transport model were conducted in this study. Contributing 40–80% to the fine particles in Shanghai, the strong transport of air pollutants carried by the frequent westerly winds is found to be the main driver of the observed pollution episodes, which brings substantial primary and secondary aerosols to the city. Compared to those originated from the local sources, the transport contributed aerosols are simulated to be less affected by the intervention measures, which can be largely attributed to the less decreased industrial and residential emissions in Jiangsu, Zhejiang, and Anhui and enhanced aerosol formation during the transport. Synergetic emission control measures, including reductions in both the traditional regulated emissions and agricultural emissions, in the Yangtze River Delta region are proved to be effective in mitigating the adverse impacts of the transport, which provide practical implications for future pollution control strategies in cities like Shanghai.

## 1. Introduction

By the end of November 2020, the outbreak of Coronavirus Disease 2019 (COVID-19) has infected over 59 million people, causing over 1 million deaths in over 200 countries (Dong et al., 2020; WHO, 2020). China enacted population-level physical distancing measures and movement restrictions to prevent the spread of the pandemic (Tian et al., 2020), simultaneously leading to negative impacts on social and economic life. Up-to-date studies suggested drastic decreases in anthropogenic emissions, especially those from traffic sectors, in China during the COVID lockdown (Bauwens, et al., 2020; Zhang et al., 2020a). The emissions of nitrogen oxide (NO<sub>x</sub> = NO + NO<sub>2</sub>) were reported to decrease by 50%–70% in eastern China compared to the pre-lockdown period (Huang et al., 2020).

The emission reductions together with corresponding atmospheric chemistry and physics processes resulted in unexpected changes in air quality in eastern China (Huang et al., 2020; Le et al., 2020; Liu et al., 2020a). Compared to those during the pre-lock period, observed concentrations of gaseous pollutants declined remarkably in Beijing-Tianjin-Hebei (BTH) and the Yangtze River Delta (YRD) regions during the COVID lockdown, with more than 60% decreases in nitrogen dioxide (NO<sub>2</sub>), and about 20%–30% in sulfur dioxide (SO<sub>2</sub>) (Huang et al., 2020; Shi et al., 2020). Yet the PM<sub>2.5</sub> (fine particulate matters with an aerodynamic diameter smaller than 2.5 μm) concentrations did not exhibit similar magnitude of decreases. Compared to the mean level during the same period in the Georgian Calendar from 2015 to 2019, observed PM<sub>2.5</sub> concentrations in Beijing increased by 55.1% during the 2020 lockdown (Le et al., 2020). The PM<sub>2.5</sub> levels in Shanghai during the period were also reported to be more than 2.5 times higher than those during the Chinese Lunar New Year (LNY) holiday in 2019 (Chang et al., 2020). Huang et al. (2020) and Le et al. (2020) found that the emission reductions resulted in increased atmospheric oxidizing capacity and then promoted the secondary aerosol formation, which was considered to be the main reason for the elevated PM<sub>2.5</sub> levels in BTH during the COVID-lock period. Comparatively, the observed enhancements in such secondary aerosol production were much smaller in YRD region (Huang et al., 2020), suggesting other factors affecting the PM<sub>2.5</sub> changes.

In addition to the emission conditions, previous studies suggested that regional transport played important roles in determining the wintertime haze pollution in YRD region (Li et al., 2019; Yang et al., 2018). During the COVID lockdown, the unfavorable meteorology was considered to exert adverse impact on the PM<sub>2.5</sub> changes (Chang et al., 2020; Wang et al., 2020), leading to 25% increase of PM<sub>2.5</sub> in Shanghai compared to those in 2019 (Liu et al., 2020b). However, more questions remain to be answered at the city level. For example, how about the contribution of meteorology relative to that of the local secondary formation? What is the influence of the COVID interventions on those contributions? How to reduce the negative impacts of meteorology on PM<sub>2.5</sub>? To answer these questions, a quantitative analysis of PM<sub>2.5</sub> changes is conducted in Shanghai during the COVID-19 outbreak in this study. The contributions from transport and local sources are assessed separately using the Weather Research and Forecasting model coupled with Chemistry (WRF-Chem), aiming to provide implications for the synergetic control of PM<sub>2.5</sub> and ozone (O<sub>3</sub>) pollution at the city level.

## 2. Methods

### 2.1. The Observational Data

Multi-year measurements of PM<sub>2.5</sub>, NO<sub>2</sub>, SO<sub>2</sub>, and O<sub>3</sub> from 2017 to 2020 in Shanghai were provided by the Shanghai Environmental Monitoring Center (SEMC). Intensive observations of PM<sub>2.5</sub> species (sulphate, nitrate, ammonium, organic carbon, and elemental carbon), NO<sub>2</sub>, carbon monoxide (CO), SO<sub>2</sub>, O<sub>3</sub>, and volatile organic species (VOCs) were also collected by SEMC at an urban site, Pudong (PD, 31.2°N, 121.5°E), in central Shanghai from January 1 to April 30, 2020. The instruments and their performance and accuracy were described by Chang et al. (2017, 2018). The meteorological elements (horizontal wind speed and direction near the surface) during the same period were provided by Baoshan Climate Observatory joining the international meteorological data exchange, described in Xu et al. (2016).

According to the different phases of the COVID-19 restrictions in Shanghai, the measurements are grouped into five periods: P1 (January 1 to 23, before the lockdown measures were conducted), P2 (January 24 to February 29, when intense government interventions were conducted), P3 (March 1 to 31, when the socioeconomic activities gradually recovered), P4 (April 1 to 30, when the social and economic life almost resumed), and P2-intense (January 24 to February 9, when the strictest restrictions were conducted). During P2-intense, the traffic and commercial activities were brought to a near stop (Shanghai Municipal People's Government, 2020a; Shanghai Municipal Health Commission, 2020a), resulting in large decreases in anthropogenic emissions, especially for NO<sub>x</sub> and VOCs (Sun et al., 2021; Zhang et al., 2020b). As the restrictions were eased during P3 and P4, the socioeconomic activities gradually resumed, resulting in gradient increases in anthropogenic emissions compared to those during P2 (Shanghai Municipal People's Government, 2020b; Shanghai Municipal Health Commission, 2020b).

## 2.2. The WRF-Chem Simulations

A fully coupled WRF-Chem model (version 3.2, <https://www2.acom.ucar.edu/wrf-chem>) improved by Tie et al. (2009) and Li et al. (2010) is used to simulate gas-phase species and aerosols in this study. The PM<sub>2.5</sub> is assembled by sulphate, nitrate, ammonium, organic carbon (OC), and primary fine particles (e.g., elemental carbon and road dust). The domain configuration, physical and chemical options, initial and lateral boundary conditions follow Zhou et al. (2017). Included in the air quality forecast ensemble system of the MarcoPolo and Partnership with China on Space Data (Panda) project (<http://www.marcopolo-panda.eu>), the performance of the applied model has been continuously and comprehensively evaluated, exhibiting good agreements with gas and aerosol observations in Shanghai and surrounding areas (Brasseur et al., 2019; Petersen et al., 2019).

To analyze the PM<sub>2.5</sub> changes and corresponding contributions of regional transport and local source during the COVID-19 pandemic, numerical simulations are performed during P2\_intense (January 24 to February 9), when the strictest government interventions were conducted in China. Baseline anthropogenic emissions are taken from the Multi-resolution Emission Inventory for China (MEIC, Li et al., 2014) for year 2010, with local adjustments following Zhou et al. (2017). The provincial emission reduction ratios during the simulation period are assigned according to Huang et al. (2020) (Table S1). Biogenic emissions are calculated online using the Model of Emissions of Gases and Aerosols from Nature (MEGAN2, Guenther et al., 2006). Sensitivity experiments with different emission scenarios are conducted as listed in Table S2.

## 3. Results

### 3.1. Air Quality Changes During the COVID-19 Pandemic in Shanghai

Figure 1 displays the observed mean concentrations of PM<sub>2.5</sub>, maximum 8h average (MDA8h) O<sub>3</sub>, NO<sub>2</sub> and SO<sub>2</sub> in Shanghai during P1–P4 from 2017 to 2020. As the strictest lockdown period (P2-intense) was similar to that of the Chinese LNY in 2020, comparisons of pollutant levels during LNY, when the anthropogenic emission reductions were noted, are also presented in the 4 years, respectively. Consistent with the emission changes due to the COVID-interventions, NO<sub>2</sub> exhibited drastic decreases of 46.2% from P1 to P2 and gradual recoveries during P3 and P4 in 2020. The mean NO<sub>2</sub> concentration during P2-2020 was 37.9% lower than the mean level during the three same periods from 2017 to 2019, indicating significant NO<sub>x</sub> emission reductions. Though exhibiting similar variations as NO<sub>2</sub>, observed SO<sub>2</sub> presented much smaller changes. The mean SO<sub>2</sub> concentrations during P2–P4 in 2020 were close to those in 2019, suggesting small impacts of COVID-interventions on SO<sub>2</sub> emissions. Different from NO<sub>2</sub> and SO<sub>2</sub>, O<sub>3</sub> exhibited continuous increases from P1 to P4 in 2020. However, similar increases could also be observed in the other three years. Compared to those in 2017–2019, observed MDA8h O<sub>3</sub> concentrations during the COVID pandemic in 2020 did not present significant increases. The result was also reported in Chen et al. (2020), suggesting the atmospheric oxidation capacity was less influenced by the COVID lockdown in Shanghai.

As suggested in recent studies (Chang et al., 2020; Liu et al., 2020b), the observed PM<sub>2.5</sub> seemed to not exhibit equivalent changes as the gas precursors during the strict COVID-lock period. Despite the 55.9% and 29.3% decreases in SO<sub>2</sub> and NO<sub>2</sub>, the observed mean PM<sub>2.5</sub> concentration during LNY in 2020 exhibited a comparable value as that in 2017. Even with similar levels of SO<sub>2</sub> and NO<sub>2</sub>, the PM<sub>2.5</sub> concentration during LNY-2020 was still 48.8% higher than that in LNY-2019. The observations also indicated that the high PM<sub>2.5</sub> concentrations were not always accompanied by increased O<sub>3</sub> levels, which was different from those reported for the North China (Huang et al., 2020; Le et al., 2020). Compared to those in 2018, observed SO<sub>2</sub>, NO<sub>2</sub>, and O<sub>3</sub> all exhibited lower concentrations in LNY-2020, but corresponding PM<sub>2.5</sub> concentration was still 16.3% higher. Thus, different mechanisms other than the emission and secondary PM formation changes were suggested to largely contribute to the enhancements of fine particles in Shanghai.

To further examine the air quality changes during the pandemic, Figure 2 presents the daily variations of gases and major PM<sub>2.5</sub> species observed at PD, an urban site, from P1 to P4 in 2020. In addition to the drastic decreases (56.3%) in NO<sub>x</sub> and slight decreases in SO<sub>2</sub> (6.0%) and CO (17.8%), VOCs at PD exhibited the second largest decreases (37.5%) during P2 compared to P1, which were consistent with the sharp declines in traffic activities due to the COVID intervention measures. Most PM<sub>2.5</sub> species exhibited similar changes as their precursors. For example, consistent with the NO<sub>x</sub> and SO<sub>2</sub> changes, nitrate exhibited the

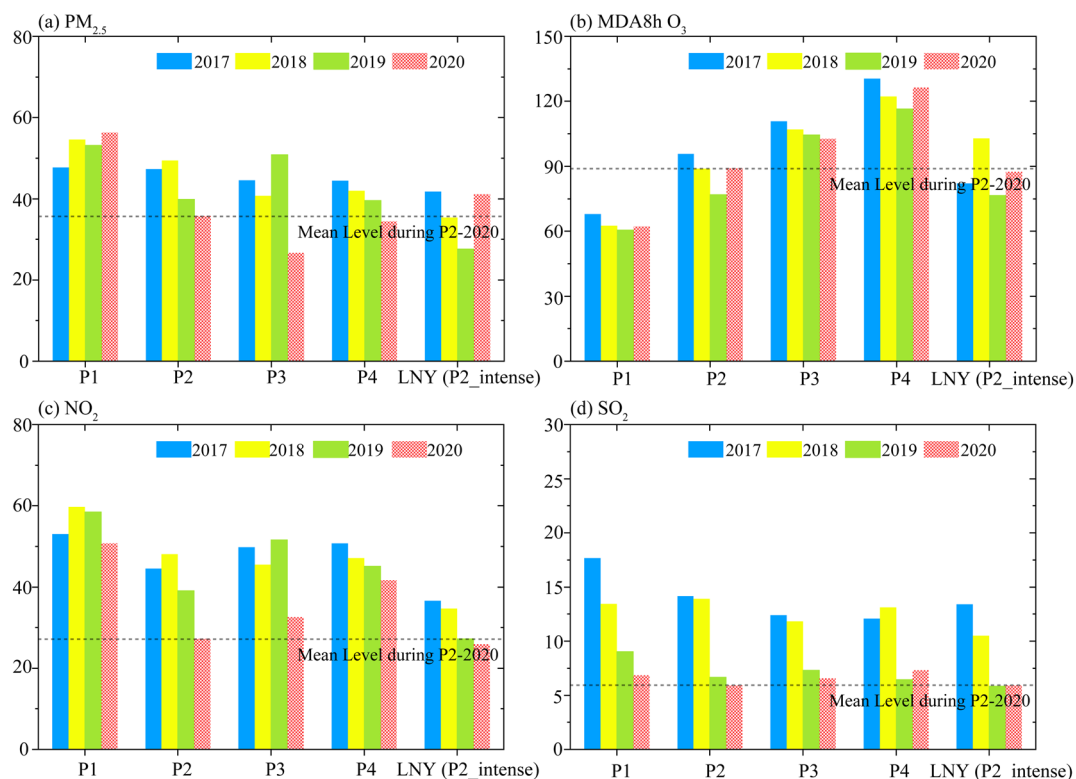


**Figure 1.** The observed mean concentrations ( $\mu\text{g m}^{-3}$ ) of  $PM_{2.5}$ , maximum 8h average (MDA8h)  $O_3$ ,  $NO_2$ , and  $SO_2$  in Shanghai during P1 (January 1 to 23), P2 (January 24 to February 29), P3 (March 1 to 31), and P4 (April 1 to 30) in 2017–2020. Also shown are the corresponding mean concentrations during the Chinese Lunar New Year (LNY, December 30 to January 16 on the lunar calendar).

largest decreases (43.8%) while sulphate presented much smaller decreases (20.5%) during P2 relative to P1. Despite the large decreases, nitrate still acted as the dominant aerosol species, accounting for 25.8% of the  $PM_{2.5}$  in urban Shanghai. The primary elemental carbon (EC) presented the second largest decline (42.6%) due to the COVID-lockdown, which was also consistent with the great emission changes (Table S1). However, compared to those during P1, OC at PD only decreased by 9.9% during P2. Considering that the drastically reduced VOCs concentrations were not conducive to the production of secondary organic aerosols, the small decreases in OC, which were also reported in Chen et al. (2020), suggested that there should be other sources contributing to the organic aerosols.

Even though the total  $PM_{2.5}$  concentrations at PD exhibited mean decreases of 37.8% during P2 compared to P1, severe pollution episodes were still observed. According to the back trajectory results (Figure S1), the observed peak  $PM_{2.5}$  concentrations during P2 were usually accompanied by remarkable transport processes affected by the westerly winds. The westerly winds tended to bring high levels of pollutants from surrounding regions, which could contribute 40%–70% to the  $PM_{2.5}$  in Shanghai (Xu et al., 2016). During P1–P4, the mean  $PM_{2.5}$  concentration under westerly winds ( $51.0 \mu\text{g m}^{-3}$ ) was about 50% higher than that under easterly winds, suggesting strong transport of pollutants from west of Shanghai. The wind rose diagrams (Figure 3) suggest that the predominant winds turned from westerly flows to easterly flows from P1 to P4. During P1–P2, the westerly winds accounted for 30%–35% of the total winds, approximately 15% higher than those during P3 and P4. The high occurrence frequency of the westerly winds further indicated that the regional transport during the first two periods was much stronger, which was conducive to the increases of  $PM_{2.5}$  concentrations in Shanghai.

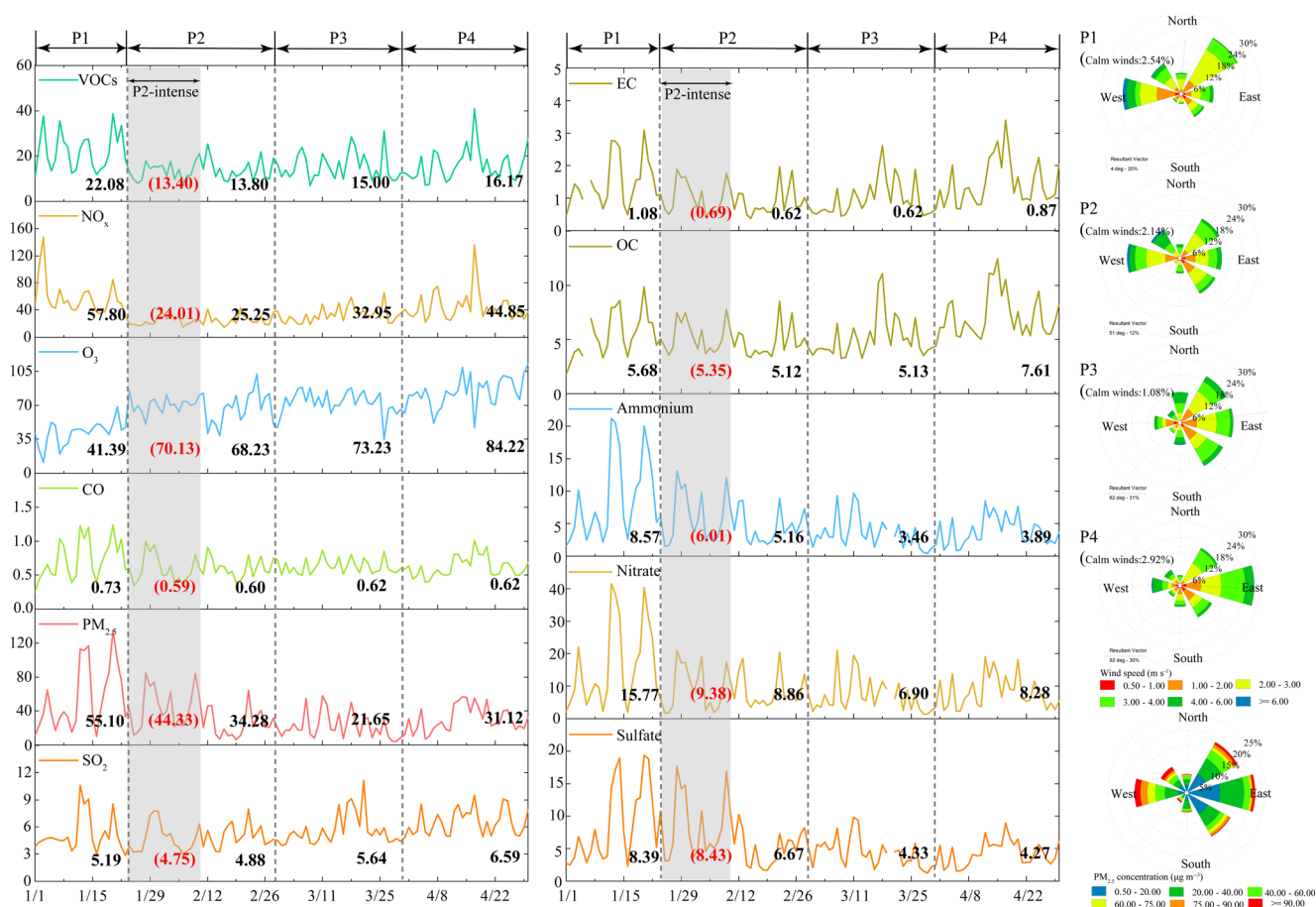


**Figure 2.** Variations of observed daily mean concentrations of gases and major  $PM_{2.5}$  components at Pudong, Shanghai. The marked numbers are the mean concentrations during P1, P2, P3, and P4, respectively. The numbers in parentheses are the mean concentrations during P2-intense. Also shown are the corresponding wind rose diagrams and period mean  $PM_{2.5}$  concentrations under different wind conditions. The units are ppbv for VOCs,  $mg\ m^{-3}$  for CO, and  $\mu g\ m^{-3}$  for other species.

### 3.2. Impacts of Regional Transport on the Air Quality Changes

To understand the unfavorable effects of regional transport on the air quality changes in Shanghai during the COVID lockdown, 14 strong transport affected days (STAD) and 17 weak transport affected days (WTAD) during P2 were selected respectively according to the back trajectories and the dominant winds. Figure 3 displays the diurnal cycles of relative changes in  $NO_2$ ,  $SO_2$ , VOCs, and  $PM_{2.5}$  at PD during STAD and WTAD, respectively compared to those during P1. In WTAD, both gases and aerosols exhibited significant decreases due to the lockdown measures, in which  $NO_2$ , VOCs, and EC presented relatively larger decreases ranging from 30% to 73%. However, in STAD, gases and aerosols exhibited different changes due to their sources.  $NO_x$  and VOCs, most of which came from local sources, were less affected by the regional transport, exhibiting comparable decreases (20%–60%) as those (30%–64%) in WTAD. In comparison,  $SO_2$  and CO present large increases during the transport. Despite the reduced emissions,  $SO_2$  and CO in STAD even exhibited enhancements up to 42.3% and 17.0%, respectively compared to those during P1, suggesting large transport induced contributions. The regional transport also led to large increases in aerosols. Under similar emission conditions, the observed concentrations of sulphate, nitrate, ammonium (SNA), and EC were almost doubled in STAD compared to those in WTAD. Corresponding OC concentrations increased by 35%–68% as well. The results indicated that the strong transport processes during the strict COVID-lockdown led to additional contributions to both aerosols and precursors, largely offsetting the efforts of emission reductions in alleviating air pollution in Shanghai.

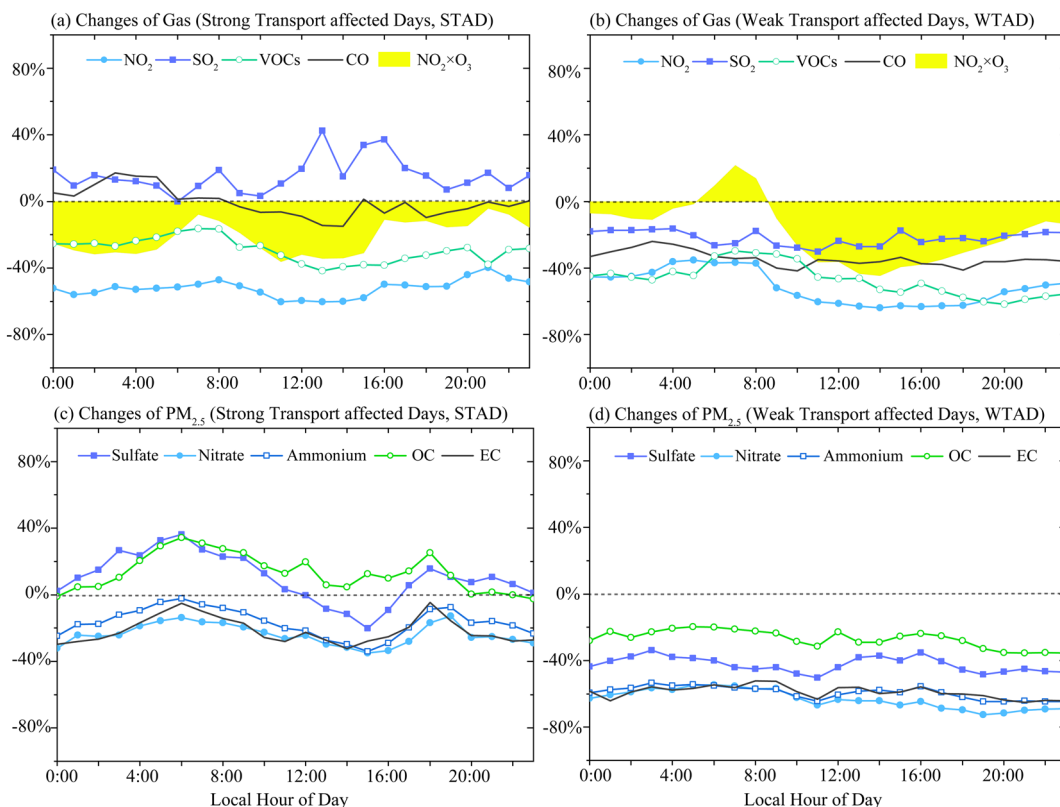


**Figure 3.** Diurnal cycles of relative changes in gases, major  $PM_{2.5}$  components, and  $NO_3$  proxy ( $NO_2 \cdot O_3$ ) at Pudong, Shanghai in strong transport affected days (STAD) and weak transport affected days (WTAD) during P2 relative to those during P1.

To examine the impacts of regional transport on the atmospheric oxidation capacity in Shanghai, Figure 3 displays the diurnal cycles of relative changes in  $NO_2 \cdot O_3$ , a proxy of  $NO_3$  radical, in WTAD and STAD, respectively compared to P1.  $NO_3$  radical is a vital oxidant for nighttime secondary PM formation and atmospheric chemistry (Brown et al., 2006; Kroll and Seinfeld, 2008; Seinfeld and Pankow, 2003). Huang et al. (2020) and Le et al. (2020) suggested that the precipitous COVID- $NO_x$  reductions had led to substantial increases in  $O_3$  and  $NO_3$  radicals, greatly promoted the formation of secondary  $PM_{2.5}$  (e.g., sulphate and nitrate) in North China. However, the  $NO_3$  radical at PD exhibited mean decreases of 21.7% and 20.4% in STAD and WTAD, respectively, compared to P1. Consistent with the observed results averaged over the YRD region (Huang et al., 2020), enhancements in  $NO_3$  radical were only observed during 5–9 a.m. in WTAD when the observed NO titration was strongest (Geng et al., 2008). The generally decreasing changes in  $NO_2 \cdot O_3$  implied that the local atmospheric oxidation capacity during P2, especially in STAD, was not conducive to the increases of the secondary PM formation in urban Shanghai. Thus, the observed enhancements in SNA, OC, and primary EC might be largely attributed to the direct transport of aerosols. Meanwhile, the secondary particles were found to be greatly enhanced during the lasting transport toward Shanghai (Chang et al., 2020). For this point of view, the regional transport was expected to increase the input of both primary and secondary  $PM_{2.5}$  to Shanghai during the lockdown, making dominant contributions to the unexpected  $PM_{2.5}$  changes.

### 3.3. Contributions of Regional Transport to the $PM_{2.5}$ Changes

To quantify the contributions of regional transport to the COVID- $PM_{2.5}$  changes, the transport and local source contributed  $PM_{2.5}$  in Shanghai during P2-intense, when the strictest interventions were conducted, are calculated separately using the WRF-Chem model. The simulated  $PM_{2.5}$  concentrations in the control run (S0) exhibit good agreements with observations (Figure S2), presenting a normalized mean bias of  $-13.0\%$  at PD during the simulation period. The correlation coefficients ( $R_s$ ) between the model results and

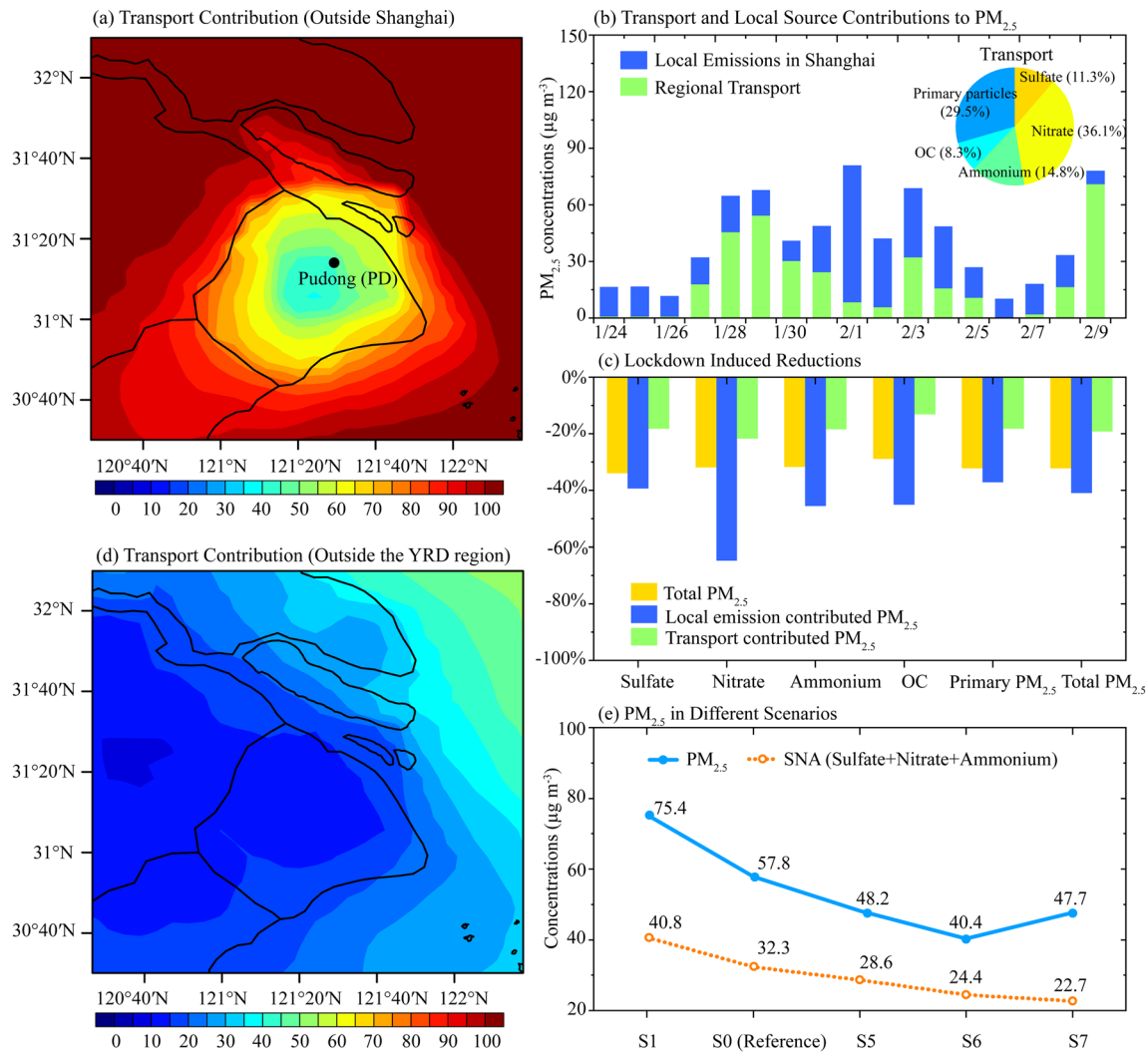


**Figure 4.** (a) Simulated distribution of the mean transport contributions (%) to  $PM_{2.5}$  concentrations from outside Shanghai during P2-intense. (b) Variations of  $PM_{2.5}$  concentrations contributed by regional transport and local emissions, respectively, and the composition of the transported  $PM_{2.5}$ . (c) Similar distribution as (a) but with contributions from outside the Yangtze Delta River region. (d) Calculated changes in  $PM_{2.5}$  and its components induced by the lockdown emission reductions during P2-intense. (e) Simulated mean concentrations of  $PM_{2.5}$  and SNA (the sum of sulphate, nitrate, and ammonium aerosols) during a strong transport affected pollution episode (January 28–30) in different emission scenarios. Calculations in (b), (d), and (e) are all averaged over the urban areas ( $30.9^{\circ}$ – $31.3^{\circ}$ N,  $121.2^{\circ}$ – $121.6^{\circ}$ E) in Shanghai.

observations are 0.72 for  $PM_{2.5}$ , and 0.56–0.79 for SNA and OC, suggesting good prediction of  $PM_{2.5}$  variations. Figure S3 suggests that the calculated percentages of nitrate (20.5%) and sulphate (16.7%) in  $PM_{2.5}$  are also fairly consistent with the observations (21.4% for nitrate and 19.3% for sulphate). Comparatively, simulated OC exhibited relatively larger discrepancy of 53.7% lower than observations, indicating underestimation of its contributions to  $PM_{2.5}$ . By comparing the sensitivity results of S0 and S2, Figure 4a suggests that the regional transport contribute to 40%–55% of the mean  $PM_{2.5}$  concentrations in urban Shanghai and 60%–80% of those in rural areas during P2-intense. For the urban region (Figure 4b), the contributions of regional transport exhibit extremely higher values during severe  $PM_{2.5}$  pollution days, reaching approximately 70%–80% in STAD (e.g., January 28–30). The results indicate that the  $PM_{2.5}$  concentrations are significantly enhanced by the strong westerly transport processes, leading to pollution episodes in spite of the drastically reduced local emissions. Though  $NO_x$  emissions are almost halved in the YRD region (Table S1), nitrate is still the dominant input species accounting for 36.1% of the transported  $PM_{2.5}$ . The proportion is followed by that (27.3%) of the transported primary fine aerosols. OC and sulphate contribute to 8.3% and 11.3%,

respectively to the transported  $PM_{2.5}$ , while the transported OC might be underestimated due to the underestimation of OC concentrations.

Figure 4c further examines the impacts of the lockdown measures on the  $PM_{2.5}$  changes by comparing the calculations with (S0–S2) and without (S1–S3) emission reductions. Due to the drastically reduced anthropogenic emissions (Table S1), the total  $PM_{2.5}$  concentrations in urban Shanghai exhibit a mean decrease of 32.2% during P2-intense, in which the transport and local source contributed parts decrease by 19.2% and 40.9%, respectively. The results indicate that the COVID-interventions effectively alleviate the  $PM_{2.5}$  pollution. However, compared to those from local sources, the transport contributed primary and secondary aerosols are simulated to be less affected by the lockdown measures. The transported SNA, OC and primary particles exhibit mean decreases of 13.2%–21.8% in urban Shanghai, which greatly mitigate the large reductions (37.1%–64.8%) in the local source contributed aerosols. To examine the sources of the transported  $PM_{2.5}$ , Figure 4d displays the calculated contribution of pollutants from outside the YRD region to the  $PM_{2.5}$  concentrations by comparing the sensitivity results of S0 and S4. Model results suggest that the regional transport from outside the YRD region only contribute 10%–15% to the mean  $PM_{2.5}$  concentrations in Shanghai during P2-intense, indicating that most transported pollutants originate from the YRD region. Compared to those in Shanghai, the anthropogenic emissions of  $SO_2$ , OC, and primary fine particles experienced relatively less reductions in other YRD regions (Jiangsu, Zhejiang, and Anhui, JZA, Table S1), most of which are from industrial and residential sources. As the lockdown was conducted during the same period as LNY in 2020, the smaller decreases in these emissions might be mainly attributed to the large migration from Shanghai to surrounding provinces, resulting in less decreases of industrial and residential activities in JZA (Shen et al., 2021). As Figure 4c shows, the transported sulphate and OC decrease by only 18.3% and 13.2%, respectively during P2-intense, which are in accordance with the relatively small emission changes. In addition, nitrate formation was reported to be greatly enhanced during the transport (Chang et al., 2020). As a result, the transported nitrate aerosols also exhibit less decreases (21.8%) compared to the local parts (64.8%) despite the similar  $NO_x$  declines in Shanghai and other YRD provinces.

Model results imply that synergetic emission control strategies over the YRD region are needed to mitigate the adverse impacts of the regional transport on the  $PM_{2.5}$  pollution in Shanghai. To examine the efficiencies of different emission reduction strategies, Figure 4e presents the simulated mean  $PM_{2.5}$  concentrations in urban Shanghai during a strong transport affected covid-pollution episode (January 28–30) under different emission scenarios (S0, S5–S7). Sensitivity results indicate that the emission reductions in surrounding provinces (JZA) are effective in decreasing  $PM_{2.5}$  concentrations in Shanghai. If similar emission reductions (approximately 50%, S5) in  $CO$ ,  $SO_2$ , VOCs, and aerosols were conducted in JZA during the lockdown, the  $PM_{2.5}$  concentrations in urban Shanghai would further decrease by 16.6% during the strong transport affected episode. In addition to the emissions listed in Table S1, ammonia ( $NH_3$ ) emission reductions are also proved to be important in mitigating the  $PM_{2.5}$  pollution. Recent studies suggested that the technical mitigation potential of agricultural  $NH_3$  was about 50% in China at present (Zhang et al., 2020b). According to the sensitivity results (S7), a further 50% cut in  $NH_3$  emissions over the YRD region can lead to additional 17.5% decreases in  $PM_{2.5}$  concentrations in urban Shanghai compared to the lockdown levels (S0), which are larger than those (16.6%) induced by the 50% synergetic emission reductions (S5). As the main components of  $PM_{2.5}$ , corresponding SNA concentrations further decrease by 29.8% in S7. The decreases in SNA are not only larger than those in S5, but also exceed those (24.4%) induced by 70% anthropogenic emission reductions in JZA (S6), suggesting that synergetic  $NH_3$  control (e.g., agricultural  $NH_3$  reductions) should be simultaneously considered so as to more effectively mitigate the adverse impacts of regional transport and alleviate the  $PM_{2.5}$  pollution in Shanghai.

#### 4. Conclusions

This study examines the adverse impacts of the regional transport on the  $PM_{2.5}$  changes in Shanghai during the COVID-19 pandemic based on a variety of WRF-Chem simulations together with intensive observations. During the strict lockdown period (P2), the  $PM_{2.5}$  species were not observed to exhibit equivalent magnitude of decreases as their gas precursors in urban Shanghai, which were found to be closely related to the strong regional transport carried by the frequent westerly winds. Though the generally decreasing atmospheric oxidation capacity were not conducive to the secondary PM formation, the regional transport



led to direct input of primary and secondary aerosols to Shanghai, largely mitigating the effects of emission reductions. Model results suggest that the regional transport contributes to 40%–55% of the mean PM<sub>2.5</sub> concentrations in urban Shanghai, and the contributions could reach over 80% in strong transport affected days. Though PM<sub>2.5</sub> pollution is effectively alleviated by the drastically reduced emissions, the transported contributed parts exhibit less decreases compared to those originated from the local sources, which could be largely attributed to the less decreased industrial and residential emissions in surrounding provinces. Synergetic emission control strategies in the YRD region are proved to be effective in decreasing PM<sub>2.5</sub> concentrations in Shanghai during the strong transport affected episode. In addition to the emissions affected by the COVID-lockdown, NH<sub>3</sub> emission reductions are also suggested to be efficient in alleviating PM<sub>2.5</sub> pollution under current emission conditions, which need to be considered in developing future strategies.

## Data Availability Statement

Model result are available at <http://doi.org/10.5281/zenodo.4420427>.

## Acknowledgments

This research was supported by the Ministry of Science and Technology of the People's Republic of China (grant no. 2019YFC0214605), Shanghai Sailing Program (grant no. 18YF1421200), and the Science and Technology Commission of Shanghai Municipality (grant nos. 19DZ1205003 and 20DZ1204006). We thank the National Centers for Environmental Prediction (US) for providing the global reanalysis data used for the WRF-Chem simulations.

## References

- Bauwens, M., Compennolle, S., Stavrou, T., Müller, J.-F., van Gent, J., Eskes, H., et al. (2020). Impact of coronavirus outbreak on NO<sub>2</sub> pollution assessed using TROPOMI and OMI observations. *Geophysical Research Letters*, *47*, e2020GL087978. <https://doi.org/10.1029/2020gl087978>
- Brasseur, G. P., Xie, Y., Petersen, A. K., Bouarar, I., Flemming, J., Gauss, M., et al. (2019). Ensemble forecasts of air quality in eastern China - Part 1: Model description and implementation of the MarcoPolo-Panda prediction system, version 1. *Geoscientific Model Development*, *12*, 33–67. <https://doi.org/10.5194/gmd-12-33-2019>
- Brown, S. S., Ryerson, T. B., Wollny, A. G., Brock, C. A., Peltier, R., Sullivan, A. P., et al. (2006). Variability in nocturnal nitrogen oxide processing and its role in regional air quality. *Science*, *311*, 67–70. <https://doi.org/10.1126/science.1120120>
- Chang, Y., Deng, C., Cao, F., Cao, C., Zou, Z., Liu, S., et al. (2017). Assessment of carbonaceous aerosols in Shanghai, China - Part 1: Long-term evolution, seasonal variations, and meteorological effects. *Atmospheric Chemistry and Physics*, *17*, 9945–9964. <https://doi.org/10.5194/acp-17-9945-2017>
- Chang, Y., Huang, K., Xie, M., Deng, C., Zou, Z., Liu, S., & Zhang, Y. (2018). First long-term and near real-time measurement of trace elements in China's urban atmosphere: Temporal variability, source apportionment and precipitation effect. *Atmospheric Chemistry and Physics*, *18*, 11793–11812. <https://doi.org/10.5194/acp-18-11793-2018>
- Chang, Y., Huang, R., Ge, X., Huang, X., Hu, J., Duan, Y., et al. (2020). Puzzling haze events in China during the coronavirus (COVID-19) shutdown. *Geophysical Research Letters*, *47*, 12. <https://doi.org/10.1029/2020gl088533>
- Chen, H., Huo, J., Fu, Q., Duan, Y., Xiao, H., & Chen, J. (2020). Impact of quarantine measures on chemical compositions of PM<sub>2.5</sub> during the COVID-19 epidemic in Shanghai, China. *The Science of the Total Environment*, *743*, 140758. <https://doi.org/10.1016/j.scitotenv.2020.140758>
- Dong, E., Du, H., & Gardner, L. (2020). An interactive web-based dashboard to track COVID-19 in real time. *The Lancet Infectious Diseases*, *20*, 533–534. [https://doi.org/10.1016/s1473-3099\(20\)30120-1](https://doi.org/10.1016/s1473-3099(20)30120-1)
- Geng, F., Tie, X., Xu, J., Zhou, G., Peng, L., Gao, W., et al. (2008). Characterizations of ozone, NO<sub>x</sub>, and VOCs measured in Shanghai, China. *Atmospheric Environment*, *42*, 6873–6883. <https://doi.org/10.1016/j.atmosenv.2008.05.045>
- Guenther, A., Karl, T., Harley, P., Wiedinmyer, C., Palmer, P. I., & Geron, C. (2006). Estimates of global terrestrial isoprene emissions using MEGAN (model of emissions of gases and aerosols from nature). *Atmospheric Chemistry and Physics*, *6*(11), 3181–3210. <https://doi.org/10.5194/acp-6-3181-2006>
- Huang, X., Ding, A., Gao, J., Zheng, B., Zhou, D., Qi, X., et al. (2020). Enhanced secondary pollution offset reduction of primary emissions during COVID-19 lockdown in China. *National Science Review*, *0*, 1–9. <https://doi.org/10.1093/nsr/nwaa137>
- Kroll, J. H., & Seinfeld, J. H. (2008). Chemistry of secondary organic aerosol: Formation and evolution of low-volatility organics in the atmosphere. *Atmospheric Environment*, *42*, 3593–3624. <https://doi.org/10.1016/j.atmosenv.2008.01.003>
- Le, T., Wang, Y., Liu, L., Yang, J., Yung, Y. L., Li, G., & Seinfeld, J. H. (2020). Unexpected air pollution with marked emission reductions during the COVID-19 outbreak in China. *Science*, eabb7431. <https://doi.org/10.1126/science.abb7431>
- Li, G., Lei, W., Zavala, M., Volkamer, R., Dusanter, S., Stevens, P., & Molina, L. T. (2010). Impacts of HONO sources on the photochemistry in Mexico City during the MCMA-2006/MILAGO Campaign. *Atmospheric Chemistry and Physics*, *10*, 6551–6567. <https://doi.org/10.5194/acp-10-6551-2010>
- Li, J., Liao, H., Hu, J., & Li, N. (2019). Severe particulate pollution days in China during 2013–2018 and the associated typical weather patterns in Beijing-Tianjin-Hebei and the Yangtze River Delta regions. *Environmental Pollution*, *248*, 74–81. <https://doi.org/10.1016/j.envpol.2019.01.124>
- Li, M., Zhang, Q., Streets, D. G., He, K. B., Cheng, Y. F., Emmons, L. K., et al. (2014). Mapping Asian anthropogenic emissions of non-methane volatile organic compounds to multiple chemical mechanisms. *Atmospheric Chemistry and Physics*, *14*, 5617–5638. <https://doi.org/10.5194/acp-14-5617-2014>
- Liu, F., Page, A., Strode, S. A., Yoshida, Y., Choi, S., Zheng, B., et al. (2020a). Abrupt decline in tropospheric nitrogen dioxide over China after the outbreak of COVID-19. *Science Advances*, *6*(28), eabc2992. <https://doi.org/10.1126/sciadv.abc2992>
- Liu, T., Wang, X., Hu, J., Wang, Q., An, J., Gong, K., et al. (2020b). Driving forces of changes in air quality during the COVID-19 lockdown period in the Yangtze River Delta Region, China. *Environmental Science & Technology Letters*, *7*(11), 779–786. <https://doi.org/10.1021/acs.estlett.0c00511>
- Petersen, A. K., Brasseur, G. P., Bouarar, I., Flemming, J., Gauss, M., Jiang, F., et al. (2019). Ensemble forecasts of air quality in eastern China - Part 2: Evaluation of the MarcoPolo-Panda prediction system, version 1. *Geoscientific Model Development*, *12*, 1241–1266. <https://doi.org/10.5194/gmd-12-1241-2019>

- Seinfeld, J. H., & Pankow, J. F. (2003). Organic atmospheric particulate material. *Annual Review of Physical Chemistry*, *54*, 121–140. <https://doi.org/10.1146/annurev.physchem.54.011002.103756>
- Shanghai Municipal Health Commission. (2020a). *Notices of Shanghai Municipal Health Commission about the Coronavirus disease 2019 prevention and control*. Retrieved from <http://wsjkw.sh.gov.cn/xwfb/20200124/fae67efb1b2048bb980461a2f42f1c2a.html>
- Shanghai Municipal Health Commission. (2020b). *Notices of Shanghai Municipal Health Commission about the Coronavirus disease 2019 prevention and control*. Retrieved from <http://wsjkw.sh.gov.cn/xwfb/20200323/3219ce0f5c1c4f7ba2af713340ab2b03.html>
- Shanghai Municipal People's Government. (2020a). *Announcements of Shanghai Municipal People's government about the Coronavirus disease 2019 prevention and control*. Retrieved from [http://www.shanghai.gov.cn/nw48539/20200826/0001-48539\\_1423599.html](http://www.shanghai.gov.cn/nw48539/20200826/0001-48539_1423599.html)
- Shanghai Municipal People's Government. (2020b). *Announcements of Shanghai Municipal People's government about the Coronavirus disease 2019 prevention and control*. Retrieved from [http://www.shanghai.gov.cn/nw48666/20200826/0001-48666\\_64001.html](http://www.shanghai.gov.cn/nw48666/20200826/0001-48666_64001.html)
- Shen, H., Shen, G., Chen, Y., Russell, A. G., Hu, Y., Duan, X., et al. (2021). Increased air pollution exposure among the Chinese population during the national quarantine in 2020. *Nature Human Behaviour*, *5*, 239–246. <https://doi.org/10.1038/s41562-020-01018-z>
- Shi, X., & Brasseur, G. P. (2020). The response in air quality to the reduction of Chinese economic activities during the COVID-19 outbreak. *Geophysical Research Letters*, *47*, e2020GL088070. <https://doi.org/10.1029/2020gl088070>
- Sun, W., Zhu, L., De Smedt, I., Bai, B., Pu, D., Chen, Y., et al. (2021). Global significant changes in formaldehyde (HCHO) columns observed from space at the early stage of the COVID-19 pandemic. *Geophysical Research Letters*, 2020GL091265.
- Tian, H., Liu, Y., Li, Y., Wu, C.-H., Chen, B., Kraemer, M. U. G., et al. (2020). An investigation of transmission control measures during the first 50 days of the COVID-19 epidemic in China. *Science*, *368*, 638–642. <https://doi.org/10.1126/science.abb6105>
- Tie, X., Geng, F., Peng, L., Gao, W., & Zhao, C. (2009). Measurement and modeling of O<sub>3</sub> variability in Shanghai, China: Application of the WRF-Chem model. *Atmospheric Environment*, *43*, 4289–4302. <https://doi.org/10.1016/j.atmosenv.2009.06.008>
- Wang, P., Chen, K., Zhu, S., Wang, P., & Zhang, H. (2020). Severe air pollution events not avoided by reduced anthropogenic activities during COVID-19 outbreak. *Resources, Conservation and Recycling*, *158*, 104814. <https://doi.org/10.1016/j.resconrec.2020.104814>
- WHO (2020). *Coronavirus disease (COVID-19) Weekly Epidemiological Update and Weekly Operational Update*. Retrieved from <https://www.who.int/emergencies/diseases/novel-coronavirus-2019/situation-reports/>
- Xu, J., Chang, L., Qu, Y., Yan, F., Wang, F., & Fu, Q. (2016). The meteorological modulation on PM<sub>2.5</sub> interannual oscillation during 2013 to 2015 in Shanghai, China. *The Science of the Total Environment*, *572*, 1138–1149. <https://doi.org/10.1016/j.scitotenv.2016.08.024>
- Yang, Y., Wang, H., Smith, S. J., Zhang, R., Lou, S., Qian, Y., et al. (2018). Recent intensification of winter haze in China linked to foreign emissions and meteorology. *Scientific Reports*, *8*, 2107. <https://doi.org/10.1038/s41598-018-20437-7>
- Zhang, R., Zhang, Y., Lin, H., Feng, X., Fu, T.-M., & Wang, Y. (2020a). NO<sub>x</sub> Emission Reduction and Recovery during COVID-19 in East China. *Atmosphere*, *11*, 433. <https://doi.org/10.3390/atmos11040433>
- Zhang, X., Gu, B., van Grinsven, H., Lam, S. L., Liang, X., Bai, M., & Chen, D. (2020b). Societal benefits of halving agricultural ammonia emissions in China far exceed the abatement costs. *Nature Communications*, *11*, 4357. <https://doi.org/10.1038/s41467-020-18196-z>
- Zhou, G., Xu, J., Xie, Y., Chang, L., Gao, W., Gu, Y., & Zhou, J. (2017). Numerical air quality forecasting over eastern China: An operational application of WRF-Chem. *Atmospheric Environment*, *153*, 94. <https://doi.org/10.1016/j.atmosenv.2017.01.020>